

SCIENTIFIC REPORTS

OPEN

A novel library of α -arylketones as potential inhibitors of α -glucosidase: Their design, synthesis, *in vitro* and *in vivo* studies

Tania Luthra¹, Rahul Agarwal¹ ³, Mamidala Estari⁴, Uma Adepally² & Subhabrata Sen¹

α -glucosidase is an essential enzyme located at the brush border of intestines. It is an important therapeutic target for type II diabetes. Herein we have designed a library of novel α -arylketones as inhibitors of α -glucosidase (yeast origin) *via* scaffold hopping and bioisosteric modification of known inhibitors of α -glucosidase. The design was validated through molecular docking that revealed strong binding interactions of the newly designed compounds against α -glucosidase. A library comprising of 15 compounds was synthesized in a combinatorial fashion, where the advanced amide intermediates were accessed through "shot gun" synthesis. The final compounds were characterized by ¹H, ¹³C-NMR and with high resolution mass spectroscopy. *In vitro* screening of the compounds against yeast α -glucosidase revealed substantial inhibition with IC₅₀s in the range of 4–10 μ M (the standard drug acarbose inhibits α -glucosidase with an IC₅₀ of 9.95 μ M). Reaction kinetics suggested mixed type inhibition. Finally, *in vivo* studies of the most active compound 3c against Streptozotocin induced male albino Wistar rats revealed that its administration in the rats for about 4 weeks lead to a highly significant ($P < 0.001$) decrease in the fasting blood glucose (FBG) compared to the untreated diabetic rats. Moreover, lower dose of 3c had better control over FBG in contrast to high-dose.

α -glucosidase is an exocyclic enzyme that hydrolyses the 1,4- α -glycosidic linkages of oligosaccharides. The oligosaccharides are then converted to monosaccharides which are then absorbed into the blood from the intestine¹. Blood carries these monosaccharides to the individual cells where they are converted into energy by the cell machinery with the help of insulin. At times the cells fail to recognize insulin or insufficient amount of insulin gets secreted from the pancreas. Consequently the monosaccharides failed to get converted to the energy and are retained in the blood, which in turn increases the blood glucose level, leading to hyperglycemia. This condition leads to type II diabetes one of the most fatal non communicable disease of the modern world². Hence α -glucosidase is an essential target for type II diabetes and their inhibitors are used to alleviate the disease³. These inhibitors bind to α -glucosidase and delay the absorption of carbohydrates from the small intestine, thereby lowering the postprandial blood glucose level⁴. In last few years various small molecules have been reported as potential inhibitors of α -glucosidase^{5–9}. For example, 5-bromo-2-arylbenzimidazole derivatives exhibited dual inhibition against α -glucosidase and urease enzymes. Additionally they are non-cytotoxic by nature¹⁰. In another report molecular modeling studies generated 3-thiazolyl coumarine derivatives as effective inhibitors against α -glucosidase, with IC₅₀ in the range of 0.12–16 μ M¹¹. A one pot multicomponent reaction involving aryl hydrazide/phenyl hydrazine and benzophenone with appropriate aryl thiocyanates and phenacyl bromide

¹Department of Chemistry, School of Natural Sciences, Shiv Nadar University, Dadri, Chithera, GautamBudh Nagar, Uttar Pradesh, 201314, India. ²Institute of Science and Technology Jawaharlal Nehru Technological University, Kukatpally, Hyderabad, Telangana, India. ³Department of Life Sciences, School of Natural Sciences, Shiv Nadar University, Dadri, Chithera, GautamBudh Nagar, Uttar Pradesh, 201314, India. ⁴Department of Zoology, Kakatiya University, Warangal-506009, Telangana, India. Correspondence and requests for materials should be addressed to U.A. (email: vedavathi1@jntuh.ac.in) or S.S. (email: subhabrata.sen@snu.edu.in)

afforded novel thiazoles which inhibit α -glucosidase with IC_{50} in the range of 9–82 μ M¹². Apart from small molecules natural product extracts have also demonstrated inhibition of α -glucosidase enzyme¹³.

Nojirimycin, Miglitol, Voglibose and Acarbose are marketed drugs for type II diabetes which target α -glucosidase enzyme^{14–17}. In general α -glucosidase inhibitors are advantageous over other antidiabetic drugs due to their localized action and minimum absorption (this subsequently reduces the systemic side effects)¹⁸. However the aforementioned drugs are quite old (discovered about 30–40 years) and suffer from disadvantages related to flatulence, abdominal pain and diarrhea due to microbial action on undigested carbohydrates¹⁹. Hence development of alternative α -glucosidase inhibitor is always a promising drug discovery endeavor. Herein we report, design of a series of α -arylketoones as novel α -glucosidase inhibitors through scaffold hopping and bioisosteric modification of known α -glucosidase inhibitors. The design was rationalized through molecular docking. The compounds were synthesized in a parallel fashion, where the advanced intermediates were synthesized *via* “shot gun” synthesis²⁰. Finally the compounds were subjected to *in vitro* screening against yeast α -glucosidase and *in vivo* screening in Streptozotocin induced male albino wistar rats, to assess their potential as candidates against type II diabetes.

Scaffold hopping is a technique where the central core of a bioactive molecule is replaced with an appropriate chemical motif, in a bid to generate a new molecule with equal or better potency compared to the original molecule²¹. This is also done to augment the selectivity (against the relevant target) and ADMET properties. For example Merck identified a piperidine based T-type Ca^{2+} inhibitors, which were later scaffold hopped to a new motif containing pyrrolidine fused with cyclopropane ring system. These newer compounds were favorable lead molecules over the piperidine class of molecules, exhibiting much better *in vivo* results²².

Bioisosteric modification is another lead optimization technique where, certain substituents in the original molecule are replaced with suitable functionalities that can potentially improve physicochemical parameters such as ADMET, pk/pd, toxicity and etc. of the original molecule²³. For example, in a bid to discover anti-inflammatory drugs acting through the selective inhibition of prostaglandin-H synthase-2 (PGHS-2) or cyclooxygenase-2 (COX-2) the scientists from Pfizer/Searle discovered a pyrazole based compound SC-58125. Despite good selectivity profile and excellent potency, this drug reported a half-life of ~200 h, thereby revealing poor susceptibility during its metabolism in the liver. Bioisosteric replacement of the methyl and the fluorine functionality in the molecule with $-NH_2$ and $-CH_3$ reduced the half-life to 8–12 h, thereby making it compatible for introducing it in the market as an anti-inflammatory agent²⁴.

Finally “shot gun” synthesis is a procedure where multiple products are generated simultaneously in a reaction. This can happen when individual reactions occur at rates sufficiently different to allow them to progress in a same reaction chamber without interference²⁵.

Results and Discussions

Design. In a bid to design novel inhibitors against α -glucosidase, we interrogated the structural features of plethora of small molecules reported in the literatures as inhibitors of α -glucosidase. We selected few molecules with moderate to good activity, which would provide us with the scope of further improving the activity through our newly designed molecule. Accordingly compounds **1a–c** and **2** were selected^{26,27}. **1a–c** are alkaloids called *Peparium Bellactams*, isolated from the branches of *Piper Umbellatum*. They exhibited moderate inhibitory activity against α -glucosidase (yeast) with IC_{50} of 30–90 μ M (Fig. 1)²⁶. Compound **2**, lowered blood glucose level in NA-STZ-diabetic mice at 10, 31.2 and 56.2 mg/Kg (Fig. 1)²⁷. A closure look at these two classes of molecules revealed topological similarity between them as depicted by fragment **A** in Scheme 1. The stilbene moiety is incorporated from **1a–c**. Bioisosteric shuffling of the imine nitrogen in **B** with oxygen resulted in scaffold **C**. Final scaffold modification involved installation of the amide functionality (inspired from **1a–c**) to generate the desired molecules **3a–o**.

Next the design of our new molecular scaffolds were rationalized by comparing the binding interaction of **3k** (a representative molecule of our library) and a homology model of α -glucosidase along with **1**, **2** and acarbose (a standard drug) (Fig. 2). The homology model was created from human maltase glucoamylase (PDBID: 2QLY, 3L4T) which exhibited strong similarity with the query sequence. The stereochemical quality of this model was validated by Ramachandran plot which revealed that ~99.3% of residue are in favored and allowed regions with only 0.7% outliers (refer SI).

From the docking interactions it was observed that compound **3k**, could potentially bind more strongly to α -glucosidase than **1** and **2** (Fig. 2). Furthermore, close scrutiny revealed comparable hydrogen bonding and hydrophobic interactions between the original molecules (**1** and **2**) and **3k** with α -glucosidase (Fig. 2). The predicted binding conformations of **1** indicate one hydrogen bond interaction with the α -glucosidase protein model where the hydroxyl group of **1** bonds with the carboxylate group of the Asp528 residues having a distance of 1.80 Å. Compound **2** indicate four hydrogen bonding interactions with residues Gly563, Ser588, Leu589 and Leu590 (Fig. 2). The three hydrogen bonds were formed between the amino group (N-H) of Ser588, Leu589, Leu 590 residues and the ring oxygen of the lactone ring with a distance of 3.44 Å, 3.04 Å and 2.14 Å respectively. The fourth hydrogen bond was observed between the amino group (N-H) of Gly563 residues and the carbonyl oxygen of the lactone moiety in **2** with a distance of 2.37 Å. Compound **2** exhibits hydrophobic interaction with the Trp288, Phe561 and Leu589 residues (Fig. 2). The binding interactions of compound **3k** involve two hydrogen bonds in which the carbonyl oxygens of compound **3k** are bonded with the amino group (N-H) of Leu589 and Leu590 respectively with a distance of 2.14 Å and 1.72 Å. Compound **3k** also displayed hydrophobic interaction with the residues Trp530 and Leu562 (Fig. 2). Finally, acarbose interacted with the homology model, through six amino acid residues *via* nine hydrogen bonds and two amino acids *via* hydrophobic interaction. The hydrophobic interactions were observed with Trp393 and Phe437. The hydrogen bonds were present between ring hydroxy groups of acarbose and the carboxylate functionality of Asp194, Ser435, Asn436, Leu589, Leu590, Ser591

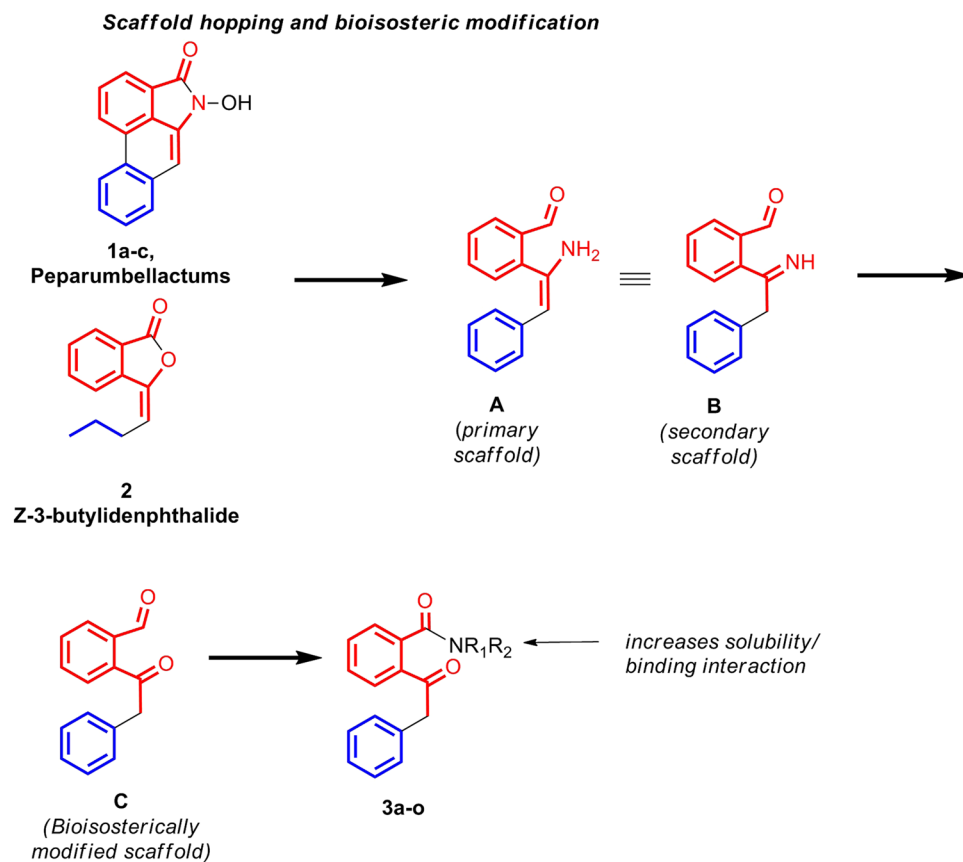


Figure 1. Design of novel α -glucosidase inhibitors by scaffold hopping and bioisosteric modification.

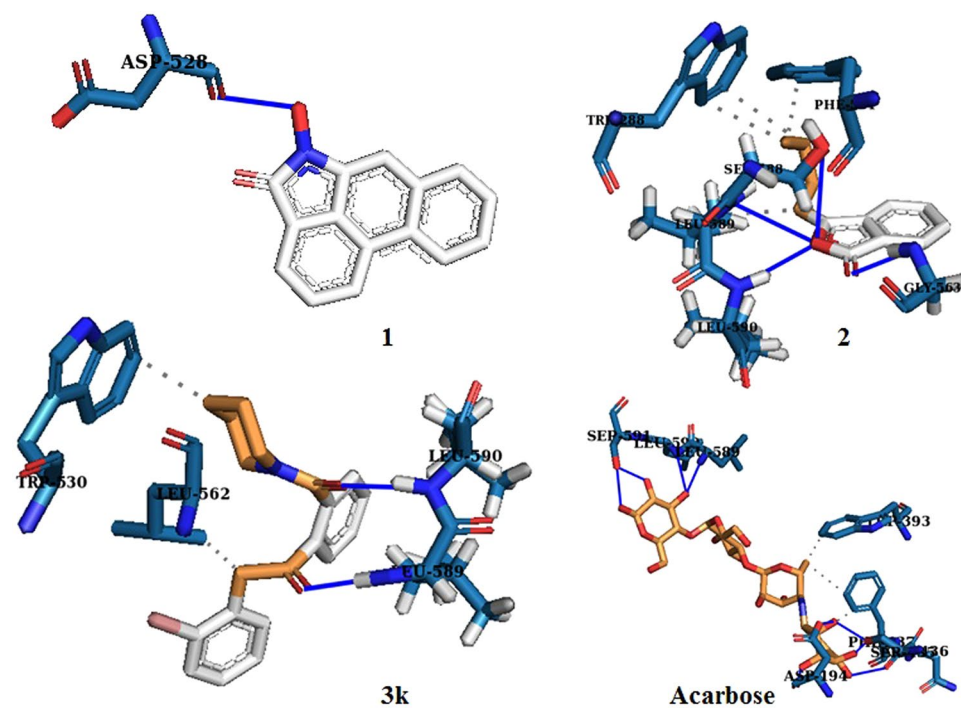


Figure 2. Molecular docking of 1, 2, 3k and acarbose with a homology model of α -glucosidase.

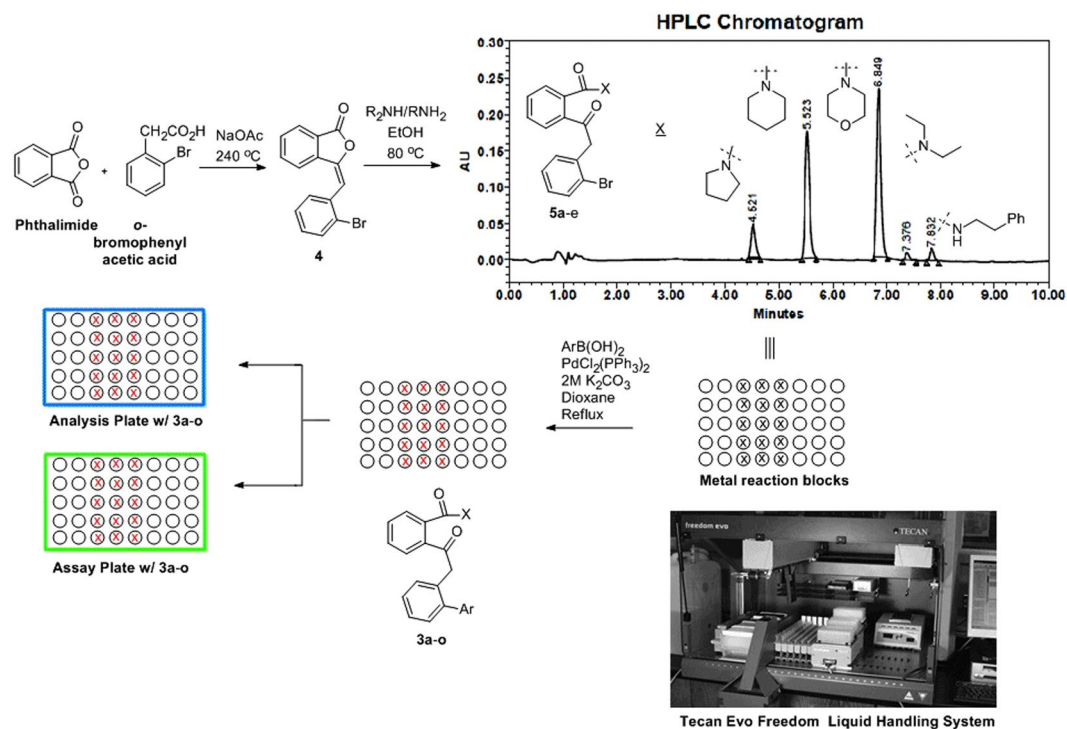
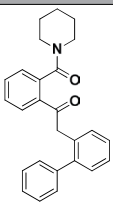
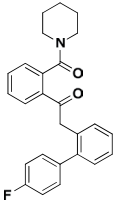
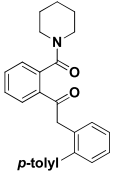
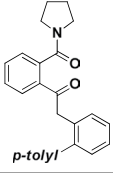
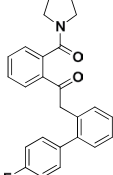
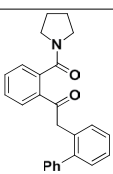
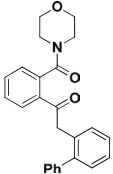
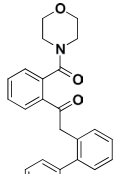


Figure 3. Synthesis of the library of compounds **3a-o**.

residues. The subsequent docking scores are -6.11 , -5.33 , -7.21 and -4.45 kcal/mol for **1**, **2**, **3k** and acarbose respectively.

Chemistry. Based on the docking results we envisioned a focused library of 15–20 members based on compound **3k**. Accordingly Knoevenagel condensation of phthalimide with *o*-bromophenyl acetic acid in sodium acetate (NaOAc) afforded compound **4** (Fig. 3). This was subjected to a “shot gun” synthesis to obtain a series of next five intermediates **3k-o**^{28,29}. A typical procedure involved dissolving five equivalents of **4** in morpholine, piperidine, pyrrolidine, diethyl amine and phenethyl amine (one equivalent each) and subsequent stirring at room temperature. The reaction was monitored by HPLC (high performance liquid chromatography) and when it indicated completion of **4** (Fig. 3), the reaction was quenched with water to remove any excess unreacted amine and was extracted with ethyl acetate. The organic layer was dried over anhydrous magnesium sulphate, evaporated and the crude was subjected to flash column chromatography (twice) for the isolation of the intermediate amides **3k-o** (Fig. 3). The final Suzuki reactions between the amides **3k-o** with appropriate boronic acids were conducted in parallel within custom made metallic reaction blocks in pre-tared reaction vessels containing 0.05 molar solution of amides **3k-o** (scale: 50–100 mg) in dioxane with palladium chloride bistriphenyl phosphine ($\text{PdCl}_2(\text{PPh}_3)_2$) and aqueous potassium carbonate (K_2CO_3) (Fig. 3). The reactions were monitored by LCMS and once it indicates complete consumption of the starting amides, the reactions were quenched and the products were extracted with ethyl acetate in a shaker. The supernatant ethyl acetate layers were transferred to a different set of pre-tared vials, evaporated under high vacuum and the net amount of compounds were deduced (Fig. 3). 2 mg of samples (including that of **3k-o**) were transferred to a 96 well analytical plate, which was subjected to HPLC analysis to assess the purity of the products. To our utmost gratification eight out of the ten compounds of **3a-j** exhibited $>95\%$ purity. The remaining two were washed multiple times with hexane to achieve the desired purity. An assay plate was also generated containing 50 μM solution of compounds in dimethyl sulfoxide. The whole operation was executed through a TecanEvo Freedom liquid handling system containing robotic arms (Fig. 3). The average yield of the analogs ranged from 79–94%. All the compounds were further characterized by ^1H , ^{13}C -NMR and high resolution mass spectroscopy.

In vitro screening and structure activity relationship studies. To assess the inhibitory effect and also the extent of selectivity our library was against α -glucosidase (yeast origin), α -fucosidase (bovine kidney origin) and α -mannosidase (jack bean origin) (in 96-well plates employing 4-nitrophenyl- α -D-glucopyranoside (PNPG) as substrate) (Table 1). The test compounds were dissolved and diluted in dimethyl sulfoxide (DMSO). They were placed in the plate along with the substrate and 10 mM of potassium sulphate buffer. They were then reacted with appropriate enzymes. After incubating the plates for ten minutes, the absorbance of the wells were measured at 430 nm. The increase in abundance (ΔA) was compared against the control i.e. buffer. The inhibitory concentrations (IC_{50} s) were computed using the standard formula ($\text{Inhibition\%} = \frac{\Delta A_{\text{control}} - [\Delta A_{\text{sample}}]}{\Delta A_{\text{control}}} \times 100$). Acarbose, is used as a standard drug for this assay (Table 1).

Compounds (structures)	Compound #s	IC ₅₀ s in μM^a		
		α -glucosidase (yeast)	α -fucosidase (bovine kidney)	α -mannosidase (jack bean)
	3a	5.93	>50	>50
	3b	5.88	>50	>50
	3c	4.50	>50	>50
	3d	5.68	>50	>50
	3e	4.93	34.43	>50
	3f	5.95	48.08	>50
	3g	5.15	>50	49.41
	3h	5.17	>50	>50
Continued				

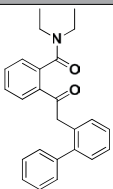
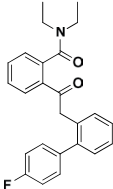
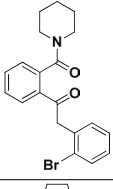
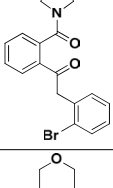
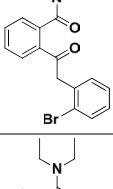
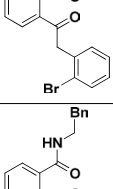
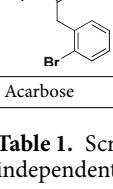
Compounds (structures)	Compound #s	IC ₅₀ s in μM ^a		
		α-glucosidase (yeast)	α-fucosidase (bovine kidney)	α-mannosidase (jack bean)
	3i	5.93	>50	23.82
	3j	5.89	>50	44.78
	3k	5.81	>50	36.21
	3l	5.20	>50	>50
	3m	10.15	>50	>50
	3n	10.13	>50	>50
	3o	6.93	>50	>50
Acarbose	—	9.95		

Table 1. Screening of compounds **3a–o** against variety of α-glycosidases. ^aIC₅₀ was determined from two independent assays, performed in duplicate.

From *in vitro* screening it is evident that the structure activity relationship (SAR) in this series of molecules is extremely constricted. In general the molecules have shown decent inhibitory activity against yeast α-glucosidase with IC₅₀ ranging from 4.5–10.2 μM. Interestingly, they have not exhibited any substantial inhibition in α-fucosidase (bovine kidney) or α-mannosidase (jack bean) indicating high selectivity of binding with α-glucosidase. The most active compound **3c** exhibited inhibition of 4.5 μM. To explain the SAR, the molecular architecture is divided into three segments. The northern most segment (N) consists of various amides, the central segment (C) is the diketoaryl moiety and finally the aromatic region in the south segment (S) (Fig. 4). From the initial SAR it is obvious that the centrally located diketoaryl moiety is essential to impart inhibition in yeast α-glucosidase. In segment N, variety of cyclic amines such as piperidine, pyrrolidine, and morpholine are well tolerated, as exemplified by low micromolar IC₅₀s of **3a–l** (Table 1). However the phenethyl amine analog **3o** was least effective. A closure look at the aromatic region in the south segment (S), revealed that other than **3k** the *o*-bromo aromatics such as **3m** and **n** are not as potent as the other aromatic compounds such as **3c–e** (10.1 →

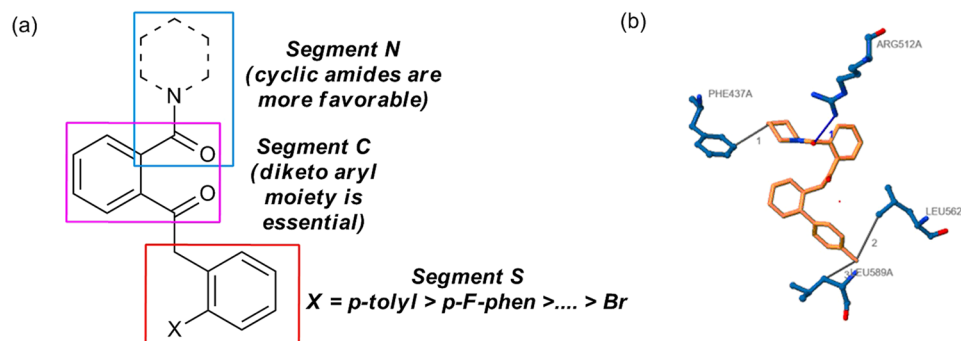


Figure 4. (a) SAR studies of our library against yeast α -glucosidase; (b) Binding interactions of **3c** with the homology model of α -glucosidase.

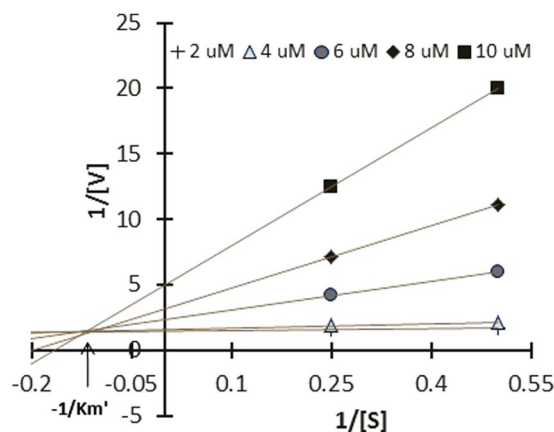


Figure 5. LB plot and secondary plot of **3c** and α -glucosidase (yeast origin) binding studies indicated a mixed type inhibition.

4.49 μM). It is noteworthy that our most active compound **3c**, was twice as active as the standard drug acarbose (IC_{50} 4.5 Vs 9.95 μM). From this initial SAR we conclude that pyrrolidine and piperidines are tolerated in segment N. The diketoaryl moiety at the center is essential and substituted (with methyl) aromatics down south (S) facilitates the activity. Furthermore, the docking study of **3c** with the homology model of α -glucosidase revealed several critical binding interactions (including one hydrogen bonding and three hydrophobic interactions) between them which explains its high inhibitory activity (Fig. 4).

Reaction kinetics. Inhibition kinetics assay of the most active compound **3c**, was performed to understand the mode of action of the compound against α -glucosidase (yeast origin). The inhibition kinetics was determined graphically by using primary (Lineweaver-Burk) and secondary plots. Figure 5, depicted the α -glucosidase inhibition kinetics plot for compound **3c** (refer SI for raw data). It revealed that all the data points on the Lineweaver-Burk plot of **3c** get intersected in the second quadrant, which indicated a mixed type of inhibition. This indicated binding of **3c** with the enzyme (α -glucosidase) as well as the enzyme-substrate (α -glucosidase-PNDP) complex. This generated two inhibition constants, K_i and K_i' (3.8 and 4.6), which were determined from the slope of the secondary plots and Y-intercept of the LB plot against the concentrations of **3c**. The smaller K_i stipulated stronger inhibition of the enzyme which further indicated the possibility of an allosteric binding site in the enzyme where **3c** can bind. One way to confirm this would be a single crystal X-ray analysis of **3c**- α -glucosidase co-crystal. This is ongoing in our lab.

In vivo studies. Male albino Wistar rats weighing between 200–240 gm each were used for the present investigation. The animals were categorized into five groups (I–V) containing three animals each ($n = 3$). Group-I is the non-diabetic control (only drug vector), group-II is the positive test control (Streptozotocin [STZ] induced), group-III is the diabetes induced group with low dose of **3c** (3.6 mg/kg of the body weight), group-IV is also a diabetes induced group administered with **3c** at higher dose (7.2 mg/kg of body weight) and finally Acarbose (a standard drug) administered (10 mg/kg of body weight) diabetes induced group V. Each animal was housed in a separate cage at a temperature of $24 \pm 3^\circ\text{C}$, with relative humidity of $65 \pm 5\%$ and a 12 h dark-light cycle.

The serum glucose level was measured in both the normal and diabetic rats on 3rd and 28th day, respectively, following the administration of **3c** and Acarbose, as positive standard. Three days after the STZ injection, the diabetic rats showed a significant ($P < 0.001$) increase in their fasting blood glucose (FBG) compared to the control group (Fig. 6b). There was a significant elevation in serum glucose, glycated haemoglobin (HbA1C) and serum

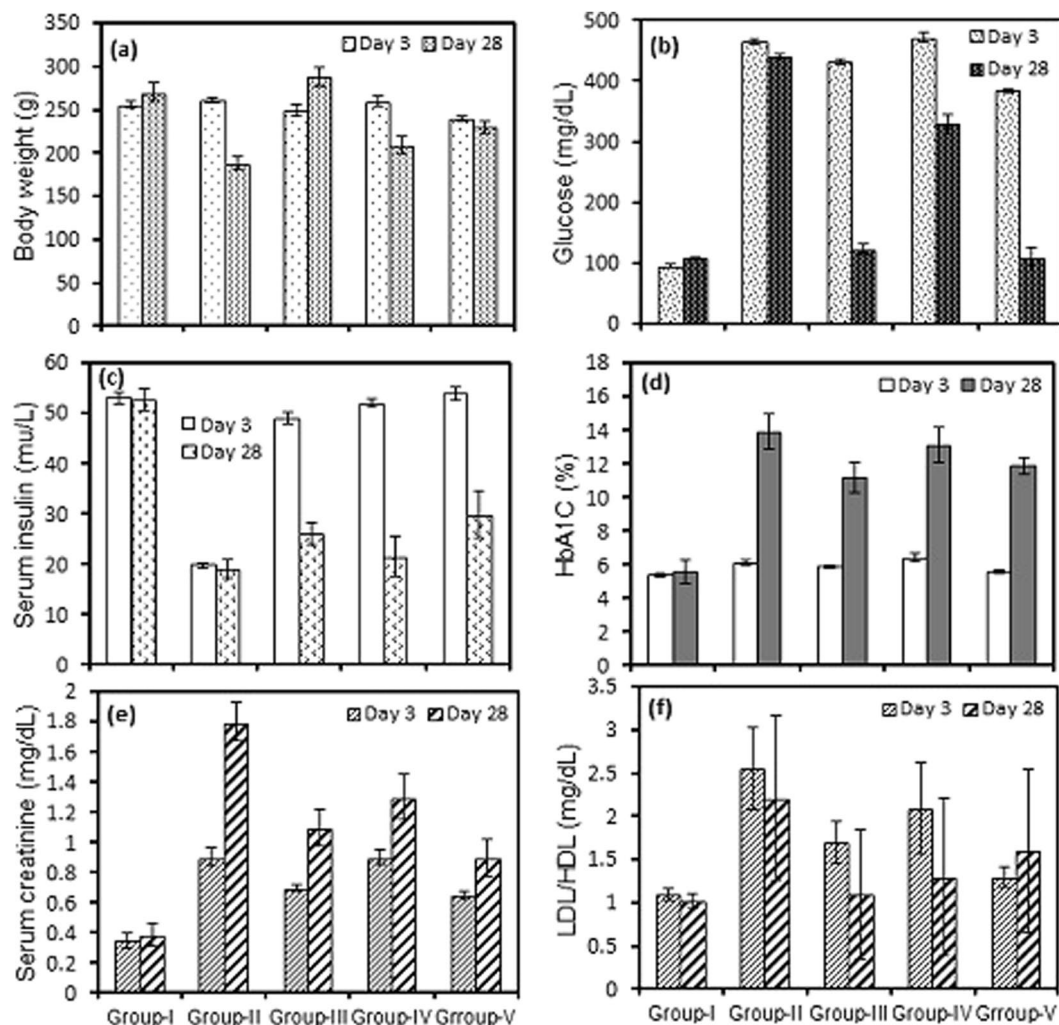


Figure 6. Effect of oral administration of 3c at doses of 3.6 (group-III) and 7.2 mgkg⁻¹ body wt. (group-IV) on (a) animal body weight; (b) serum glucose; (c) serum insulin; (d) HbA1C; (e) serum creatinine; (f) LDL/HDL ratio. Acarbose was administered at dose of 10 mgkg⁻¹ body wt. for treating diabetes positive control rats (group-V). Each column represents mean ± SD for three rats (n = 3). Streptozotocin was used for inducing diabetes. The level of significance for the investigation was in between (P = 0.05–P = 0.001).

creatinine while the serum insulin levels were significantly decreased in diabetic rats (Fig. 6b,c,d,e respectively). The administration of 3c for about 4 weeks revealed a highly significant ($P < 0.001$) decrease in the FBG (fasting blood glucose) compared to the untreated diabetic rats. Moreover, lower dose of drug had better control over FBG in contrast to high-dose (Fig. 6b). This indicated that the drug is only an inhibitor of α -glucosidase at intestinal microvilli and perhaps at higher dosage of the drug was inhibiting α -glucosidase activity at an increased level and eventually decreasing the levels of blood glucose which resulted in the activation of hyperglycemic hormones for the maintenance of glucose levels^{30,31}. Insulin levels dropped sharply after the administration of Streptozotocin, however, moderate improvement in the level of insulin was observed with 3c after the treatment period (Fig. 6c). Further, the histological profile revealed atrophy of islet cells of pancreas in diabetic rats (Fig. 7a–c) and these animals exhibited moderate periportal inflammation in liver while mild inflammation was observed with rats treated with 3c (Fig. 8a,b). As the blood glucose levels were controlled in response to 3c, there could have been an opportunity for the pancreatic cells to repair in about 28 days which could lead to the improvement in insulin levels (Fig. 6c). The same was depicted in the histological changes associated with pancreatic cells i.e., shrinkage of β -cells in diabetic control while improved β -cell population in the presence of 3c (Fig. 7a–c). Interestingly, insulin levels had not reached that of control values even after 28 days which might be due to the accumulation of toxic intermediates^{32,33}.

The HbA1c increased significantly in diabetic rats, but, the response to the drug was not enough to make a change in their levels in comparison to that of nondiabetic rats (Fig. 6d) (at the end of the test period). Generally, the glycated haemoglobin is degraded over a period of three months, but, the change in HbA1c (from 11.9 → 13.9%) ($P < 0.05$) might be attributed to the formation of certain new population of RBC which were getting glycated at the lowering levels of glucose^{34,35}. Elevation in the values of LDL to HDL ratio was observed with diabetes

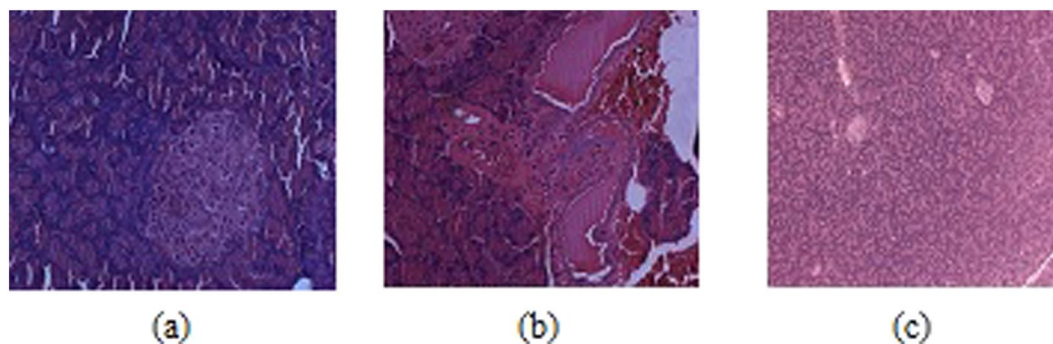


Figure 7. Histology of pancreas (a) normal case; (b) diabetic positive control, and (c) test compound high-dose treated.

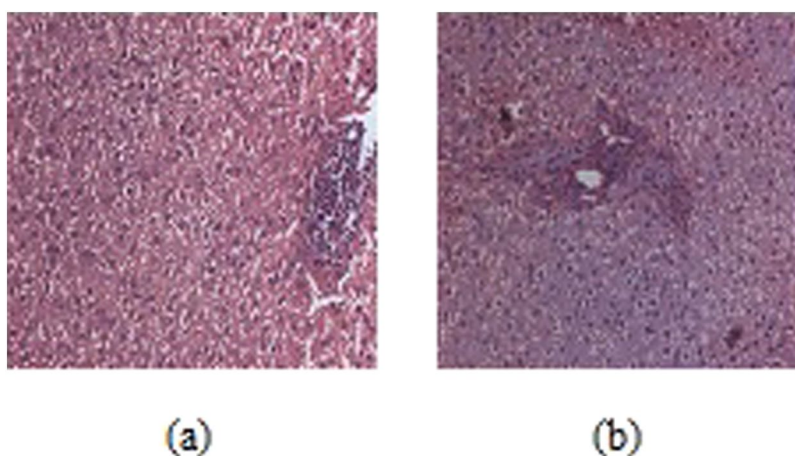


Figure 8. Histology of liver (a) diabetic positive control; (b) test compound high-dose treated.

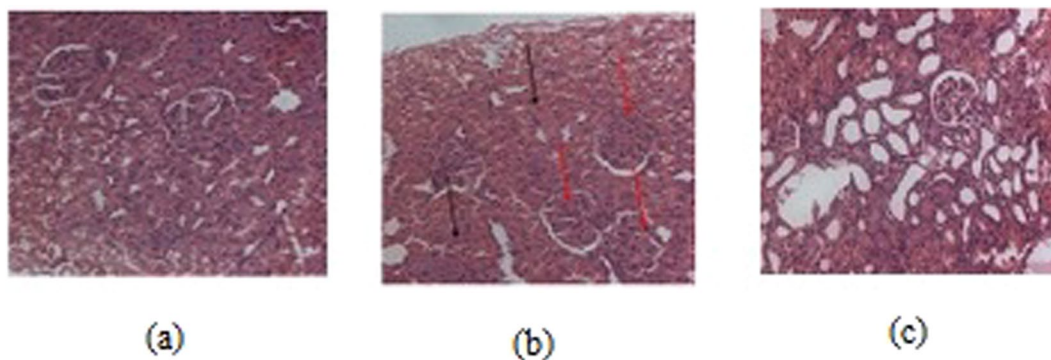


Figure 9. Histology of kidney (a) diabetic positive control; (b) test compound high-dose treated.

for about 28 days, but, the increase of this ratio was moderately high with low dosage of drug and it was slightly higher in case of high-dose which was controlled by the levels of secreted insulin (Fig. 6f). The insulin resistance observed after induction of diabetic condition led to the decrease in uptake of glucose which was excreted in the urine. This could result in increased breakdown of fat deposits and eventual increase of triglycerides, cholesterol and its esters^{36,37}. Additionally, there could be decreased synthesis of apoprotein part of lipoprotein which could have the increased levels of VLDL compared to HDL³².

The serum creatinine clearance is based on the severity of diabetic condition^{38,39}. Streptozotocin caused damage to nephrons and in turn facilitated serum clearance of creatinine from the destruction of muscle mass in severe diabetes with insulin resistance^{40,41}. In the present investigation, there was an augmented levels of serum creatinine in the diabetic condition and moderately high levels of clearance with test animals (Fig. 6e). The change in the volume of skeletal muscle (Fig. 6a) and its concomitant effect on causing insulin resistance was also

reflected in the serum creatinine levels. The condition was severe with interstitial inflammation and nephritis observed with diabetic control (Fig. 9a–c).

Conclusion

Herein we have reported the discovery of a library of α -aryl ketones, as novel inhibitors of α -glucosidase (yeast). The design of these molecules included scaffold hopping and bioisosteric modification of lesser known natural product inhibitors of α -glucosidase i.e. **1** and **2**. The combinatorial strategy of compound generation involving a “shot-gun” synthesis of intermediates afforded a fifteen membered focused library (**3a–o**). *In vitro* screening of these molecules against α -glucosidase (yeast), α -fucosidase (bovine kidney) and α -mannosidase (jack bean) exhibited selective low micromolar inhibition of our compounds against α -glucosidase. The most active compound **3c** inhibited with an IC_{50} of 4.5 μ M (acarbose, a standard drug inhibited α -glucosidase with an IC_{50} of 9.95 μ M). Reaction kinetics study of **3c**, recommended it to be a mixed inhibitor which further indicated an allosteric binding of **3c** against α -glucosidase. *In vivo* study of **3c**, against male albino Wistar rats revealed that a lower dosage of 3.6 mg/kg of **3c** had better control over FBG (300 mg/dl \rightarrow 120 mg/dl) in comparison to higher dosage (7.6 mg/kg), with minimal toxicity. This further suggested that **3c** may inhibit α -glucosidase at intestinal micro villi. Finally **3c** was docked against a homology model of α -glucosidase, to understand the putative binding sites. This proof of concept study provided fundamental information to begin an elaborate structure activity relationship campaign to identify a more potent α -arylketone as α -glucosidase inhibitors which eventually can be transformed into a preclinical candidate against type II diabetes.

Materials and Methods

Chemistry. Commercially available reagents and solvents were used without further purification. All reactions were monitored by thin-layer chromatography (TLC) using TLC plates (60 F254). The yields are not optimized. The purity of all compounds was over 95% as analyzed with an Agilent ZORBAX Eclipse Plus C18 (4.6 mm \times 50 mm, 3.5 mm) reverse phase column, detecting with UV absorbance (254 nm). Purification of reaction products was carried out by flash chromatography using an InterchimPuriFlash[®] 450 purification system with Interchim silica gel columns. ¹H NMR and ¹³C NMR spectra were recorded with tetramethylsilane (TMS) as internal standard at ambient temperature unless otherwise indicated Bruker 400 MHz for ¹H NMR and 100 MHz for ¹³C NMR. Chemical shifts are reported in parts per million (ppm) and coupling constants are reported as Hertz (Hz). Splitting patterns are designated as singlet (s), broad singlet (bs), doublet (d), triplet (t). Splitting patterns that could not be interpreted or easily visualized are designated as multiple (m). The Mass Spectrometry analysis was done on the 6540 UHD Accurate-Mass QTOF LC/MS system (Agilent Technologies) equipped with Agilent 1290 LC system obtained by the Dept. of Chemistry, School of Natural Sciences, Shiv Nadar University, Uttar Pradesh 201314, India.

Enzymatic assays. The inhibitory effect of the synthesized compounds on α -glucosidase (yeast origin), α -fucosidase (bovine kidney origin) and α -mannosidase (jack bean origin) inhibitory activity was determined in 96-well plates employing the substrate PNPG and 4-nitrophenyl α -D-glucopyranoside according to the procedure previously reported by Ferreres *et al.*⁴². Prior to use, all test compounds were solubilised in solvent, dimethylsulfoxide (DMSO), and then further diluted in DMSO to acquire the desired final maximum test concentration. Briefly, each well in 96-well plates contained 100 μ L of 2 mM 4-nitrophenyl α -D-glucopyranoside (PNP-G) in 10 mM potassium phosphate buffer (pH 7.2) and different test concentrations (2–10 μ M). The reaction was initiated by the addition of 5 μ L of the enzyme solution (0.1 IU per well). α -glucosidase (yeast), α -fucosidase (bovine kidney) and α -mannosidase (jack bean) were purchased from Sigma Aldrich, Bangalore. The plates were incubated at 37 °C for 10 min. The absorbance was measured spectrophotometrically at 430 nm (Spectra Max M5e micro plate reader). The increase in absorbance (ΔA) was compared with that of the control (buffer instead of test compound) to compute the inhibitory concentrations (IC_{50}) which was determined from two independent assays, performed in duplicate. Acarbose, an illustrious inhibitor of α -glucosidase was employed as positive control. Inhibition (%) = $(\Delta A_{\text{control}} - \Delta A_{\text{sample}}) / \Delta A_{\text{control}} \times 100$. The concentration of compound required to obtain 50% inhibition of α -glucosidase activity under the assay conditions was defined as the IC_{50} value.

Inhibition kinetics. The kinetic mode of inhibition of the highest active compounds against α -glucosidase was determined by preparing a series of test solutions in which the concentration of the respective substrate was varied in the presence of different concentrations of the inhibitors (10–50 μ M). The mode of inhibition (i.e. competitive, non-competitive, uncompetitive or mixed-type) of the screened compounds was determined on the basis of the inhibitory effects on K_m (dissociation constant) and V_{max} (maximum reaction velocity) of the enzyme³⁶. These studies were computed using the primary (Lineweaver–Burk plot) plots, which are the double reciprocal plots of enzyme reaction velocities (1/V) versus substrate concentrations (1/[S]). Analysis of the same data by secondary plots of slope versus [inhibitor] and Y-intercept versus [inhibitor] were also performed. The Lineweaver–Burk (LB) equation follows as:

$$V = \frac{V_{\text{max}}[S]}{K_m \left[1 + \frac{[I]_0}{K_i} \right] + [S] \left[1 + \frac{[I]_0}{K'_i} \right]}$$

Animal. Male albino Wistar rats weighing between 200–240 g each were used for the present investigation. The animals were categorized into five groups (I–V) of three each ($n = 3$), while each one was housed in a separate cage at a temperature of 24 ± 3 °C, with relative humidity of $65 \pm 5\%$ and a 12 h dark-light cycle. They were housed and handled in Biosafety Level 2 (BSL2) animal facilities at University College of Pharmaceutical Sciences,

Kakatiya University, Warangal, Andhra Pradesh, India and were provided with a standard pellet diet of laboratory and water with continuous monitoring. Actual drug administration was begun after 72 h of diabetic induction by streptozotocin (STZ). The test drug acarbose, a known α -glucosidase inhibitor were administered orally every day for about 28 days soon after the food was completed by the animal. All protocols were reviewed prior to the start of the experiment by an independent ethical review board at University College of Pharmaceutical Sciences, Kakatiya University and approved to be in accordance with the license for animal experiments issued by The Animal Experiments Inspectorate (License no. 1820/GO/Re/S/CPCSEA).

Induction of Type 2 diabetes. Diabetes was induced postprandial in the rats (Group II-V) by a single intraperitoneal (I.P) injection of freshly prepared Streptozotocin (60 mg kg^{-1} body wt.) in 0.1 M sodium citrate buffer of pH 4.5. Non-diabetic control rats (group-I) were received an I.P injection of buffer alone. Diabetes was confirmed after 72 h of STZ induction by assaying the blood glucose levels. The rats having blood glucose higher than 11 mmol L^{-1} were considered to be diabetic and selected for further study.

Determination of biochemical parameters and weight of the animal. For the determination of biochemical parameters, the animals were kept under fasting overnight and peripheral blood was drawn for the assays. The tests were carried out using commercial kits and following the manufacturer's instructions. At the end of test period of 28 days, the animals under fasting conditions were anesthetized and sacrificed. Blood and tissues were stored for further biochemical and histological studies. Each animal in every group was tested for body weight, blood glucose, insulin, creatinine, Hb1Ac, lipid profiles.

Statistical analysis. The results were expressed as mean \pm standard deviation ($M \pm SD$) for three rats in each group. The differences between treated and control groups were assessed by one way analysis of variance (ANOVA) using MINITAB (Version. 14). The values of $p < 0.05$ were considered to show the statistical significance.

Molecular docking. *Homology modeling.* The sequence of alpha-glucosidase was downloaded from Uniprot (ID: P10253). Blastp against protein data bank database was performed in order to identify the template for sequence alignment. Human Maltase-Glucoamylase (PDB ID: 2QLY, 3L4T) were showing good similarity to our query sequence. Residues starting from 89 are aligning to these PDB and showing 44% identity. So we select these two protein structure to model alpha-glucosidase using homology modelling. The homology model of alpha-glucosidase was built using Modeller v9.14. Three models were generated using Modeller v9.14 and model having best DOPE score is selected for further refinement. Modelled structure consist of certain loops structure that are further refined using ModLoop server. The energy of the refined model was minimized using maestro v10 using Force Field OPLS2005. The stereochemical quality of this model is validated by Ramachandran plot. More than 99.3% residues are in favored and allowed regions and only 0.7% (6 residues) are in outlier region.

Preparation of modelled alpha glucosidase protein structure. Protein preparation was performed using protein preparation wizard of maestro v10 in which assign bond orders, addition of hydrogens, create di-sulfide bonds were done. After that H-bond assignment were optimize using PROPKA at pH 7.0. Finally the energy of the protein were minimized using OPLS2005 force field.

Ligand preparation. The 2D structures of the compounds were build using MOE-Builder tool. After this various 3D conformation was search using conformational search tool in MOE. The conformation with least energy was selected for docking studies.

Docking. For docking studies both the modelled structure and template structure (PDB ID: 3L4T) were aligned and the centroid coordinates of the complex ligands in the crystal structure (PDB ID: 3L4T) were used as the center of the docking site. A grid of $60 \times 60 \times 60$ with 0.375 \AA were constructed around the docking area using Autogrid v 4.2 software. Docking analysis were done using Autodock v 4.2 software in which top 10 docked conformation were taken using Genetic Algorithm. Each docking calculation consist of 25×10^6 energy evaluations with 250 population size. A mutation rate of 0.02 and a crossover rate of 0.8 were used to generate new docking trials.

References

1. Bruni, C. B., Sica, V., Auricchio, F. & Covelli, I. Further kinetic and structural characterization of the lysosomal α -D-glucosidase glucohydrolase from cattle liver. *Biochim. Biophys. Acta* **212**, 470–477 (1970).
2. Maki, K. C. *et al.* High-viscosity hydroxypropylmethyl cellulose blunts postprandial glucose and insulin responses. *Diabetes Care* **30**, 1039–1043 (2007).
3. Wild, S., Roglic, G., Green, A., Sicree, R. & King, H. Global prevalence of diabetes: estimates for the year 2000 and projections for 2030. *Diabetes Care*. **27**, 1047–1053 (2004).
4. Eichler, H. G., Korn, A., Gasic, S., Prison, W. & Businger, J. The effect of a new specific α -amylase inhibitor on post-prandial glucose and insulin excursions in normalsubjects and Type 2 (non-insulin-dependent) diabetic patients. *Diabetologia* **26**, 278–281 (1984).
5. Arshad, T. *et al.* Syntheses, *in vitro* evaluation and molecular docking studies of 5-bromo-2-aryl benzimidazoles as α -glucosidase inhibitors. *Med. Chem. Res.* **25**, 2058–2069 (2016).
6. Javaid, K. *et al.* 2-Arylquinazolin-4(3H)-ones: A new class of α -glucosidase inhibitors. *Bioorg. Med. Chem.* **23**, 7417–7421 (2015).
7. Ali, F. *et al.* Hydrazinyl arylthiazole based pyridine scaffolds: Synthesis, structural characterization, *in vitro* α -glucosidase inhibitory activity, and *in silico* studies. *Eur. J. Med. Chem.* **138**, 255–272 (2017).
8. Taha, M. *et al.* Synthesis, α -glucosidase inhibitory activity and *in silico* study of tris-indole hybrid scaffold with oxadiazole: As potential leads for the management of type-II diabetes mellitus. *Bioorg. Chem.* **74**, 30–40 (2017).

9. Abbasi, M. A. *et al.* Synthesis of (E)-N'-[1-(2,4-Dihydroxyphenyl)ethylidene]Substituted Hydrazides as Possible α -glucosidase and butyrylcholinesterase Inhibitors. *J. Chem. Soc. Pak* **39**, 248–253 (2017).
10. Arshad, T. *et al.* 5-Bromo-2-Aryl benzimidazole Derivatives as Non-Cytotoxic Potential Dual Inhibitors of α -Glucosidase and Urease enzymes. *Bioorg. Chem.* **72**, 21–31 (2017).
11. Salar, U. *et al.* Syntheses of new 3-thiazolyl coumarin derivatives, *in vitro* α -glucosidase inhibitory activity, and molecular modeling studies. *Eur. J. Med. Chem.* **122**, 196–204 (2016).
12. Khan, K. M. *et al.* Synthesis, *In Vitro* α -Glucosidase Inhibitory Activity and Molecular Docking Studies of New Thiazole Derivatives. *Bioorg. Chem.* **68**, 245–258 (2016).
13. Yin, Z., Zhang, W., Feng, F., Zhang, Y. & Kang, W. α -Glucosidase inhibitors isolated from medicinal plants. *Food Science and Human Wellness* **3**, 136–174 (2014).
14. Niwa, T. *et al.* Novel glycosidase inhibitors, nojirimycin B and D-mannonic- δ -lactam. *Isolation, structure determination and biological property.* *J. Antibiot* **37**, 1579–1586 (1984).
15. Joubert, P. H., Foukaridis, G. N. & Bopape, M. L. Miglitol may have a blood glucose lowering effect unrelated to inhibition of α -glucosidase. *Eur J. Clin. Pharmacol.* **31**, 723–724 (1987).
16. Kawamori, R. *et al.* Voglibose Ph-3 Study Group. Voglibose for prevention of type 2 diabetes mellitus: a randomized, double blind trial in Japanese individuals with impaired glucose tolerance. *Lancet* **373**, 1607–1614 (2009).
17. Joubert, P. H., Venter, H. L. & Foukaridis, G. N. The effect of miglitol and acarbose after an oral glucose load: a novel hypoglycaemic mechanism. *Br. J. Clin. Pharmacol.* **30**, 391–396 (1990).
18. Balfour, J. A. & McTavish, D. Acarbose. *An update of its pharmacology and therapeutic use in diabetes mellitus.* *Drugs* **46**, 1025–1054 (1993).
19. Chiasson, J. L. *et al.* Acarbose for prevention of type 2 diabetes mellitus: The STOP-NIDDM randomised trial. *Lancet* **359**, 2072–2077 (2002).
20. Orita, A., Nagano, Y., Nakazawa, K. & Otera, J. Shotgun Process: A Practical treatment for simultaneous multiple reactions. *Synlett.* **5**, 599–602 (2000).
21. Tsunoyama, K., Amini, A., Sternberg, M. J. E. & Muggleton, S. H. Scaffold hopping in drug discovery using inductive logic programming. *J. Chem. Inf. Model.* **48**, 949–957 (2008).
22. Yang, Z.-Q. *et al.* Discovery of 1,4-substituted piperidines and selective inhibitors of T-type calcium channels. *J. Med. Chem.* **51**, 6471–6477 (2008).
23. Lima, L. M. & Barreiro, E. J. Bioisosterism: A useful strategy for molecular modification and drug design. *Curr. Med. Chem.* **12**, 23–49 (2005).
24. Robertson, D. W. & Fuller, R. W. Central serotonin receptors: opportunities for drug discovery. *Annu. Rep. Med. Chem.* **23**, 49–58 (1988).
25. Nagano, Y., Orita, A. & Otera, J. Combined lewis acid catalysts in shotgun process: a convenient synthesis of the female sex pheromone of the red-bollworm moth. *Tetrahedron* **58**, 8211–8217 (2002).
26. Tabopda, T. K. *et al.* Bioactive aristolactams from Piper umbellatum. *Phytochemistry* **69**, 1726–1731 (2008).
27. Brindis, F., Rodríguez, R., Bye, R., González-Andrade, M. & Mata, R. (Z)-3-Butylenephthalide from *Ligusticum porteri*, an α -Glucosidase Inhibitor. *J. Nat. Prod.* **74**, 314–320 (2011).
28. Nagano, Y., Orita, A. & Otera, J. Unusual Carbonyl Differentiation in the Lewis acid-Catalyzed Allylation of Aldehydes with Tetraallyltin. Applications to Parallel Recognition and Shotgun Process. *J. Bull. Chem. Soc. Jpn.* **76**, 2183–2189 (2003).
29. Lirag, R. C. & Miljanić, O. Š. Four acid-catalyzed dehydration reactions proceed without interference. *Chem. Comm.* **50**, 9401–9404 (2014).
30. Qinna, N. A. & Badwan, A. A. Impact of streptozotocin on altering normal glucose homeostasis during insulin testing in diabetic rats compared to normoglycemic rats. *Drug Des. Devel. Ther.* **9**, 2515–2525 (2015).
31. Husni, A. & Purwanti, D. & Ustadi. Blood Glucose Level and Lipid Profile of Streptozotocin-induced Diabetes Rats Treated with Sodium Alginate from *Sargassum crassifolium*. *Journal of Biological Sciences* **16**, 58–64 (2016).
32. Lim, E. L. *et al.* Reversal of type 2 diabetes: normalisation of beta cell function in association with decreased pancreas and liver triacylglycerol. *Diabetologia* **54**, 2506–2514 (2011).
33. Cheng, C. W. *et al.* Fasting-Mimicking Diet Promotes Ngn3-Driven β -Cell Regeneration to Reverse Diabetes. *Cell* **168**, 775–788 (2017).
34. Bunn, H. F. & Gabbay, K. H. & Gallop, P. M. The glycosylation of hemoglobin: relevance to diabetes mellitus. *Science* **200**, 21–27 (1978).
35. Higgins, P. J. & Bunn, H. F. Kinetic Analysis of the Nonenzymatic Glycosylation of Hemoglobin. *J. Biol. Chem.* **256**, 5204–5208 (1981).
36. Kakadiya, J., Shah, M. & Shah, N. J. Effect of nobivolol on serum diabetic marker and lipid profile in normal and streptozotocin-induced diabetic rats. *Res. J. Pharm., Biol. and Chem. Sci.* **1**, 329–334 (2010).
37. Andallu, B., Vinay Kumar, A. V. & Varadacharyulu, N. Ch. Lipid abnormalities in streptozotocin-diabetes: Amelioration by *Morus indica* L. Cv Suguna leaves. *Int. J. Diabetes Dev. Ctries.* **29**, 123–128 (2009).
38. Howard, B. V. Lipoprotein metabolism in diabetes mellitus. *J. Lipid Res.* **28**, 613–628 (1987).
39. Harita, N. *et al.* Lower Serum Creatinine Is a New Risk Factor of Type 2 Diabetes-The Kansai Healthcare Study. *Diabetes Care* **32**, 424–426 (2009).
40. Sivajothi, V., Dey, A., Jayakar, B. & Raj Kapoor, B. Antihyperglycemic property of Tragicacannabina in streptozotocin-induced diabetic rats. *J. Med Food* **10**, 361–365 (2007).
41. Zafar, M., Naeem-ul-Hassan Naqvi, S., Ahmed, M. & Kaimkhani, Z. A. Altered Kidney Morphology and Enzymes in Streptozotocin Induced Diabetic Rats. *Int. J. Morphol.* **27**, 783–790 (2009).
42. Ferreres, F. *et al.* Bauhinia forficata link authenticity using flavonoids profile: relation with their biological properties. *Food Chem.* **134**, 894–904 (2012).

Acknowledgements

This work was supported by Shiv Nadar University. We thank S. Patil at Shiv Nadar University for his assistance with HRMS experiments.

Author Contributions

S.S. designed the work and compiled the manuscript; T.L. carried out the synthesis. R.A. executed the molecular docking experiments. U.A. and M.E. executed the *in vitro* and *in vivo* studies. S.S. edited, revised and supervised the overall research work progress and revised the manuscript. All authors reviewed the manuscript.

Additional Information

Competing Interests: The authors declare that they have no competing interests.

Publisher's note: Springer Nature remains neutral with regard to jurisdictional claims in published maps and institutional affiliations.



Open Access This article is licensed under a Creative Commons Attribution 4.0 International License, which permits use, sharing, adaptation, distribution and reproduction in any medium or format, as long as you give appropriate credit to the original author(s) and the source, provide a link to the Creative Commons license, and indicate if changes were made. The images or other third party material in this article are included in the article's Creative Commons license, unless indicated otherwise in a credit line to the material. If material is not included in the article's Creative Commons license and your intended use is not permitted by statutory regulation or exceeds the permitted use, you will need to obtain permission directly from the copyright holder. To view a copy of this license, visit <http://creativecommons.org/licenses/by/4.0/>.

© The Author(s) 2017